



Universiteit
Leiden
The Netherlands

Structural changes in single chromatin fibers induced by tension and torsion

Meng, H.

Citation

Meng, H. (2014, October 9). *Structural changes in single chromatin fibers induced by tension and torsion. Casimir PhD Series*. Retrieved from <https://hdl.handle.net/1887/29020>

Version: Not Applicable (or Unknown)

License: [Leiden University Non-exclusive license](#)

Downloaded from: <https://hdl.handle.net/1887/29020>

Note: To cite this publication please use the final published version (if applicable).

Cover Page



Universiteit Leiden



The handle <http://hdl.handle.net/1887/29020> holds various files of this Leiden University dissertation

Author: Meng, He

Title: Structural changes in single chromatin fibers induced by tension and torsion

Issue Date: 2014-10-09

Chapter 4

Torsional stress controls the folding and unfolding of the chromatin fiber¹

In eukaryotic cells, DNA exists as chromatin fibers with different degrees of compaction. Folding and unfolding of chromatin plays a key role in gene regulation. However, the structural changes of a compacted chromatin fiber induced by torsional stress are poorly understood. Here we studied the stability of single supercoiled chromatin fibers, reconstituted on tandem repeats of 601 nucleosome positioning sequence. By applying tension and torsion with magnetic tweezers, we find that the fiber has a strong asymmetric response to supercoiling. Negative supercoiling stabilizes the fiber against unfolding. Positive supercoiling can be absorbed by the fiber. This anisotropy of the fiber reflects the chirality of a left-handed helix. When the force exceeds ~ 2.5 pN, the fiber unfolds, unwrapping one turn of DNA. The level of unfolding is regulated by supercoiling. An equilibrium statistical mechanics model based on chromatin topology and elasticity is presented, which captures the full complexity of chromatin folding and unfolding at different degrees of supercoiling. These results reveal for the first time the effects of supercoiling on a folded chromatin fiber and present a new quantitative model of chromatin supercoiling.

¹The contents of this chapter are based on : H. Meng and J. van Noort. “Torsional stress controls the folding and unfolding of the chromatin fiber”, manuscript in preparation.

4.1 Introduction

In eukaryotic cells, genomic DNA is organized in chromatin, a DNA-protein complex which results in a formidable compaction of DNA in the nucleus. The basic unit of chromatin is the nucleosome. Both the structure of DNA and the structure of nucleosome are known from X-ray crystallography. DNA forms a right-handed helix with 10.4 basepairs (bp) per helical turn [1]. The nucleosome consists of 147 bp of DNA wrapped 1.7 times around a wedge-shaped octamer of histone proteins in a left-handed superhelix [2]. Nucleosomes are connected by short DNA segments (linker DNA), typically 10 to 90 bp long, forming an array of nucleosomes with a diameter of about 10 nm. These arrays are thought to fold into chromatin fibers by short-range interactions between neighboring nucleosomes. In vitro, under physiological salt conditions, these fibers thicker fibers have a diameter of 30 nm, and are commonly known as the 30-nm fiber [3]. However, the higher order structure of the 30-nm fiber is controversial.

It is becoming clear that native chromatin structures are not nearly as uniform as those formed by reconstitution in vitro [4]. The structure of the chromatin fiber is sensitive to the length of linker DNA, the salt conditions, histone modifications and linker histones [5, 6]. Understanding chromatin structure is therefore complicated and it is unlikely that a “one-model-fits-all” solution to the problem exists. Furthermore, recent studies suggest that there may not be an higher order structure such as the 30-nm fiber but that chromatin in vivo rather folds into 10-nm fibers [7–9]. Chromatin compaction modeling work based on Hi-C data unfortunately doesn’t have the resolution to reveal such details [10, 11]. These studies demonstrated, by modeling, that chromatin compaction as measured by Hi-C techniques is insensitive for changes of the model from a 10-nm fiber to a 30-nm fiber.

The function of chromatin is not only to compact DNA, but also to control gene regulation. Transcription regulation involves next to a plethora of post transcriptional modifications and chromatin remodellers [12] also the effects of supercoiling [13]. During transcription, RNA polymerase (RNAP) generates large torsional stress on DNA, which is estimated to be seven DNA supercoils per second [14]. A common model to describe the RNAP elongation is the “twin supercoiled domain” model, in which the RNAP moves along the DNA helix and generates positive supercoiling (overwound DNA) ahead and negative supercoiling (underwound DNA) behind [15]. Following this model, one hypothesis [16, 17] is that positive supercoiling ahead of the RNAP will

destabilize nucleosomes, and negative supercoiling behind it will promote reassembly of nucleosomes. Recently, a psoralen based cross-linking technique was introduced to measure the local DNA supercoiling density genome wide [18, 19]. These results clearly show that the genome has separate domains with various degrees of supercoiling, supporting the idea that supercoiling is dependent on transcription, with active genes being more negatively supercoiled than inactive genes. High-resolution genome-wide nucleosome mapping also [17] suggest indirectly that positive torsional stress contributes to such destabilization of nucleosomes. However, there is no direct data on how a chromatin fiber responds to supercoiling.

Single-molecule techniques such as magnetic and optical tweezers provide powerful tools to study the effects of supercoiling. The effect of supercoiling on naked DNA is widely studied, and so is the mechanism of transcription on bare DNA [20]. However, *in vivo*, RNAP encounters DNA folded into chromatin fibers consisting of arrays of nucleosomes rather than naked DNA. Hence, the effects of supercoiling have to be considered in the context of chromatin, but this is poorly understood so far [21]. A recent study demonstrated the mechanical stability of single nucleosomes under torsion [22]. Interestingly, torque was shown to have only a moderate effect on nucleosome unwrapping. The chromatin fiber's response to torque may be quite different. Though supercoiling effects on chromatin fibers were first investigated at forces below 0.5 pN [23, 24], which is significantly lower than the DNA unwrapping force about of 3~5 pN, these experiments could therefore not reveal the effect of torque on nucleosome unwrapping. Moreover, these experiments were done at salt conditions much lower than physiological buffer conditions. The data was interpreted as a chiral transition from a left-handed nucleosome to a right-handed reversome. Because of the buffer conditions, these results could not show how folded chromatin fibers unfold by supercoiling and therefore neglected all nucleosome-nucleosome interactions.

Previously, we showed that the chromatin fibers reconstituted on the 601 sequence repeats with 50 bp linker DNA fold in accordance with the one start solenoid model [25]. Although the model has been questioned [26], one needs additional, more detailed data to resolve this discussion. The chirality of such a solenoidally folded fiber has direct implications on the mechanical properties of the fiber. Here we focus on the effects of supercoiling on the stability of the higher order structure of the fiber. We performed a comprehensive investigation of force spectroscopy on torsionally constrained chromatin fibers, under physiological buffer conditions and at different degrees of su-

percoiling. The torsionally constrained fiber has an anisotropic response to torsion. We show that the fiber does not unfold until forces exceed 2.5 pN, and has an end-to-end distance which corresponds to the fiber being stretched to a single file of stacked, interacting nucleosomes. Above this force, the unfolding of the fiber depends on the degree of supercoiling. Positive supercoiling facilitates the unfolding, but superfluous positive supercoiling refolds the fiber. We developed a torsional spring model for the chromatin fiber that captures the anisotropy of the fiber to supercoiling. We demonstrate that the chromatin fiber folds in a left-handed helix. Interestingly, this interpretation is consistent with very early diffraction studies of the fiber's chirality [27]. Our model captures all unfolding and refolding events in a quantitative manner. These findings give a detailed structural insight in how a chromatin fiber responds to supercoiling and directly test the "twin supercoiled model", yielding a better understanding of the role of chromatin during transcription.

4.2 Results

4.2.1 Torsionally unconstrained chromatin fibers

Before describing the structural changes in a chromatin fiber under torsional stress, we first review the elasticity of torsionally unconstrained chromatin fibers. A force-extension (F-E) curve of a torsionally unconstrained chromatin fiber reconstituted with 25 nucleosomes is shown in Fig. 4.1A. The fiber has about 1 kb of DNA handles on each side of the chromatin fiber. At low forces ($F < 0.5$ pN), the largest part of the increase in extension is due to the entropic elasticity of these DNA handles [28, 29]. A linear increase in extension is observed at intermediate forces (0.5 pN $< F < 2.5$ pN). In this part of the F-E curve, the elasticity of the fiber can be described by a Hookean spring [25]. Near 3 pN, a force plateau occurs, as nucleosomes in the fiber unfold into an array of singly wrapped nucleosomes (Fig. 4.1B).

The entire F-E curve can be described by a statistical mechanics model that takes into account the elasticity of the DNA and chromatin fiber, as well as the conformational changes of the nucleosomes, as shown before. In Chapter 3, we show that an intermediate state of the nucleosome between the unfolded fiber and the fully unwrapped nucleosome exists. To simplify the analysis, we combine these two conformations in a single transition. Fitting this model to the data yields a stretch modulus of the fiber,

$s_f \approx 0.5 \text{ pN}$, an unfolding energy $G_u \approx 18.5 k_B T$ and an elongation per unfolded nucleosome of 20 nm, corresponding to DNA unwrapping of about 58 bp. All the parameters are scaled per nucleosome and are summarized in Table 4.1.

4.2.2 Torsionally constrained chromatin fibers

Figs. 4.1C and 1E show the F-E curves for a chromatin fiber containing 25 nucleosomes, similar to the fiber in Fig. 4.1A, but torsionally constrained by multiple bonds between the DNA and the bead and the glass surface. Interestingly, compared to the torsionally unconstrained chromatin fiber, at $\Delta Lk = 0$, no force plateau occurs around 3 pN, but the extension increases linearly up to 4 pN. When decreasing the excess linking number from $\Delta Lk = 0$ to $\Delta Lk = -20$, the extension of the fiber decreased at forces below 1.8 pN. Between 1.8 pN and 4 pN, the extension increased linearly with force, independent of ΔLk .

To understand the response of folded chromatin fibers to supercoiling, it is important to separate the changes in extension of the DNA handles from the compliance of the fiber itself. F-E curves of bare DNA without nucleosomes are shown in Fig. S1 as comparison. Negative supercoiling results in plectonemes in the DNA, which reduce the extension of the tether [30, 31]. Like in the case of a bare DNA molecule, we observe a reduction of the extension of the fiber. This should be attributed mostly to the response of the DNA handles supercoiled into plectonemes. This plectonemic DNA transfers into melted and twisted DNA when increasing the force up to 1.8 pN. The net result is an extension that is equivalent to that of torsionally unconstrained DNA. Apparently, the DNA handles, rather than the fiber, absorb negative supercoiling.

Interestingly, when positive twist is applied, we observed hardly any change in extension compared to the torsionally unconstrained chromatin fiber at forces below 2.5 pN. This is remarkable because the presence of a 25 nucleosomes chromatin fiber, appears to prevent the 2 kb of DNA handles to form plectonemic DNA, as it does for negative twist. Above 2.5 pN, the force plateau, which is indicative of fiber unfolding, appears as more positive twist is applied, like in the case of torsionally unconstrained fibers. A maximum extension occurs at $\Delta Lk = 20$. When more twist is applied, the extension of the plateau reduces again, which is, as we will show below, due to fewer nucleosomes unfolding.

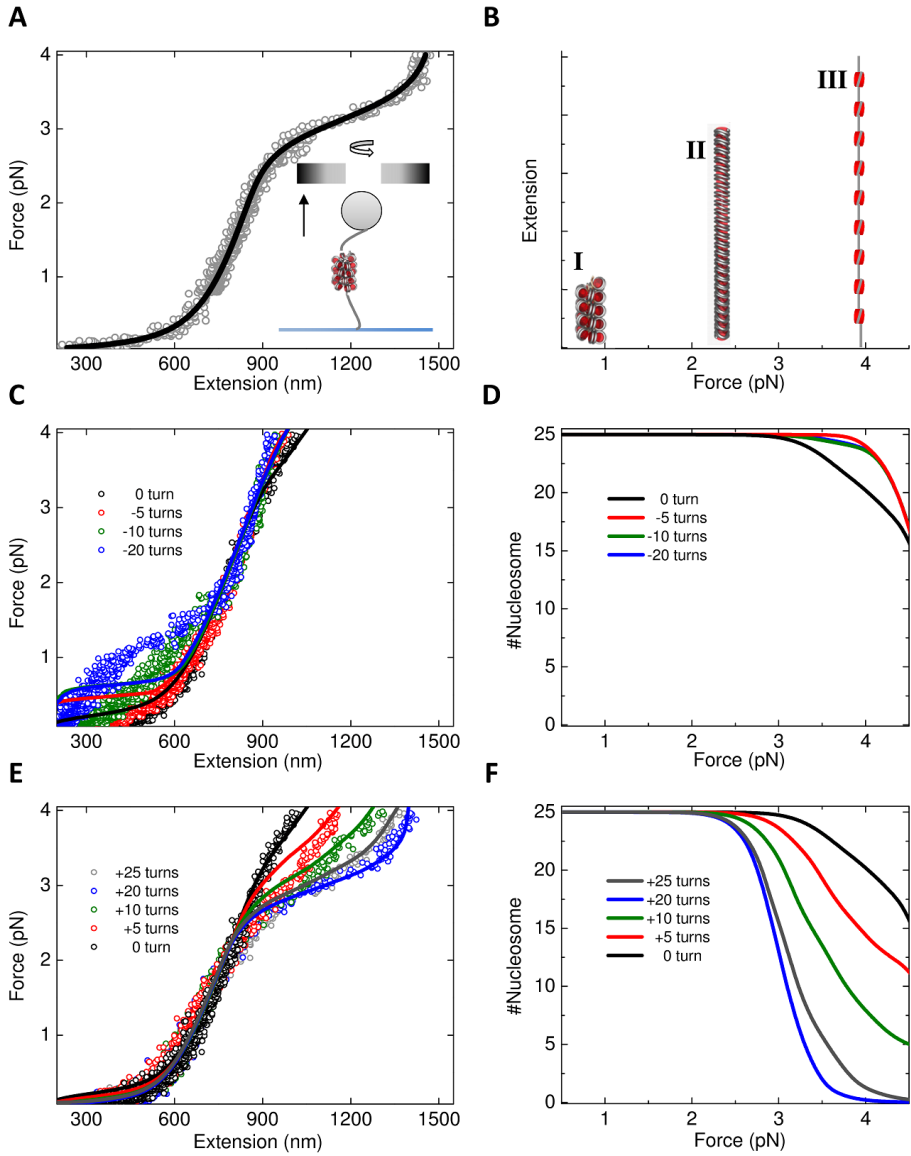


Figure 4.1: Pulling single torsionally (un)constrained chromatin fibers. (A) Force-extension curve for a torsionally unconstrained chromatin fiber reconstituted with 25 nucleosomes. The solid line is a statistical mechanics model that describes the fiber as a Hookean spring and the DNA handles as a Worm-like-chain (see Supplemental Information). Inset: Experimental setup: a single compacted chromatin fiber with DNA handles (~ 1 kb each), is tethered between a $1 \mu\text{m}$ bead and a cover-glass. Tension and torsion on the fiber is controlled by moving or rotating the magnets above the bead. (B) Schematic illustration of a chromatin fiber's conformational changes with increasing tension. I: low force regime, nucleosomes are folded into a 30-nm fiber; II: intermediate force regime, the fiber is stretched to a single stack of nucleosomes; III: high force regime, the fiber unfolds to form an array of nucleosomes that have only a single turn of wrapped DNA. (C) Force-extension curves for a single torsionally constrained chromatin fiber with 25 nucleosomes at various degrees of negative supercoiling (dots). The solid lines are global fits to Equation 4.6. (D) The number of folded nucleosomes calculated by the model as a function of force under negative supercoiling. (E) Force-extension curves for the same fiber at various degrees of positive supercoiling. Global fits are drawn with solid lines. (F) The calculated number of folded nucleosomes under positive supercoiling.

Thus, excess positive supercoiling appears to be absorbed by the fiber, whereas negative supercoiling stabilizes the fiber's structure. Positive supercoiling can be stored in the fiber at low forces, and restores chromatin fiber unfolding at high forces in torsionally constrained fibers. These are clear indications that the fiber is not folded in an isotropic structure, but rather displays features that point to a left-handed superhelix that can handle some undertwisting, but cannot be over-twisted.

4.2.3 A quantitative statistical mechanics model for unfolding a supercoiled chromatin fiber

To quantify the interpretation above, we extended our statistical mechanics model for a torsionally unconstrained chromatin fiber. We consider a Hookean torsional spring, yielding an elastic energy G_{fiber} [28, 32, 33]:

$$G_{fiber} = \frac{1}{2} \frac{s_f}{Nz_f^0} (\Delta z_{fiber})^2 + \frac{1}{2} \frac{c_f}{Nz_f^0} (2\pi Lk_{fiber})^2 + \frac{g_f}{Nz_f^0} (\Delta z_{fiber}) (2\pi Lk_{fiber}) \quad (4.1)$$

where s_f is the stretch modulus of the fiber; c_f is the twist modulus, and g_f is the twist-stretch coupling factor. N is the total number of fully folded nucleosomes and

z_f^0 is the length of fiber in the absence of force, which is about 1.7 nm per nucleosome [5, 34]. Δz_{fiber} is the extension change of the fiber by pulling and twisting. The total extension of the folded fiber is $z_{fiber} = Nz_f^0 + \Delta z_{fiber}$. Lk_{fiber} is the linking number of fiber. The force and torque on the fiber are calculated from the derivative of the free energy to the extension and to the linking number [35]:

$$\begin{aligned} F &= \frac{s_f}{Nz_f^0} \Delta z_{fiber} + \frac{g_f}{Nz_f^0} (2\pi Lk_{fiber}) \\ \Gamma_{fiber} &= \frac{c_f}{Nz_f^0} (2\pi Lk_{fiber}) + \frac{g_f}{Nz_f^0} \Delta z_{fiber} \end{aligned} \quad (4.2)$$

The entire tether in our experiment consists of a part of chromatin fiber and a part of DNA handles. The mechanical properties of the DNA handles (free energy G_{DNA} , extension of DNA z_{DNA} , and the torque Γ_{DNA}) are described by twisted, plectonemic and melted conformations [36] (see Supplemental Information). The excess linking number of the tether is distributed between the two parts, with the torque considered equal in both parts of the tether. To capture the anisotropy of the fiber in response to twist, we include a linking number Lk_{fiber}^0 per nucleosome, yielding a total twist in the fiber,

$$Lk_{fiber} = N \times Lk_{fiber}^0 + \Delta Lk_{fiber} \quad (4.3)$$

Combining Equation 4.2, 4.3 and the elasticity of DNA (details in Supplemental Information) yields the elastic response of a DNA-fiber tether:

$$z(F, \Delta Lk, N) = z_{DNA}(F, \Delta Lk_{DNA}) + z_{fiber}(F, \Delta Lk_{fiber}, N), \quad (4.4)$$

for forces small enough not to rupture the fiber.

The force-induced rupturing of the nucleosomes in the fiber yields nucleosomes with one turn wrapped of DNA. The linking number that is constrained by the nucleosome in the fiber will redistribute along the tether when such a rupture event takes place. The elasticity of the resulting unfolded nucleosome is defined by the linker DNA plus the length of DNA that is released from the nucleosome. In addition, an amount of free energy G_u for each nucleosome is released when nucleosome-nucleosome and nucleosome-DNA interactions break. Note that we describe the unfolding of the fiber as a single transition, as opposed to our previous modeling, in order to keep the model as simple as possible. We can numerically calculate the partition function for a finite number of nucleosomes:

$$Z = \sum_{i=0}^N \binom{N}{i} \exp\left(-\frac{G_{DNA} + G_{fiber} + iG_u - Fz(F, \Delta Lk + iLk_{fiber}^o, i)}{k_B T}\right), \quad (4.5)$$

i is the number of nucleosomes that is unfolded, and $\binom{N}{i}$ is a binomial coefficient that takes the degeneracy of nucleosome unfolding into account. The expected value of total extension at a certain force and an excess linking number is then given by:

$$\langle z(F, \Delta Lk, N) \rangle = Z^{-1} \sum_{i=0}^N z(F, \Delta Lk + iLk_{fiber}^o, i) \binom{N}{i} \exp\left(-\frac{G_{DNA} + G_{fiber} + iG_u - Fz}{k_B T}\right) \quad (4.6)$$

4.2.4 Comparison between data and model

We performed a global fit to our data for forces between 1.0 pN to 4.0 pN, and excess linking numbers ΔLk ranging from -5 to 25. The elastic parameters of the chromatin fiber were fit and those of DNA were fixed to known values. (solid lines in Figs. 4.1C and E). We obtain $s_f = 0.48 \pm 0.02$ pN, $c_f = 3.4 \pm 0.2$ pN nm², $g_f = 0.03 \pm 0.01$ pN nm. An unfolding energy $G_u = 17.80 \pm 0.04 k_B T$ was found, very similar to that of a torsionally unconstrained fiber, shown in Fig. 4.1A. The linking number per nucleosome yields $Lk_{fiber}^o = -0.81 \pm 0.01$. Our model also recovers the number of folded nucleosomes at different forces and excess linking numbers. It can be seen in Figs. 4.1D and F that all the nucleosomes stay in the folded conformation at $F < 2.5$ pN. The change in extension of the tether at forces larger than 2.5 pN can be attributed to an increase in the number of unfolded nucleosomes. Interestingly, adding more positive supercoiling ($\Delta Lk > 21$ for 25 repeats) reduces the extension of the tether, suggesting that fewer nucleosomes unfold when excessive positive supercoiling is applied.

At low forces ($F < 1.0$ pN) and negative supercoiling, the model deviates from the data. This is remarkable as we obtain very good agreement between data and model for bare DNA (see Fig. S1). The reduced extension that we observe for low forces and negative supercoiling may indicate a more complex interplay among fiber structure, plectonemes and melting bubbles in the DNA handles. Apart from this small region in force and excess linking number, we obtain an excellent agreement between the model

	Linking number per basepair/ nucleosome Lk^o	Stretch modulus s (pN)	Twist-stretch coupling g (pN nm)	Twist modulus c (pN nm ²)	Unfolding energy G_u ($k_B T$)
B-DNA	0.1	1000	-90	440	----
25x 197 torsionally unconstrained	----	0.46±0.05	----	----	18.31±0.04
(25x197) global	-0.81±0.01	0.48±0.02	0.03±0.01	3.4±0.2	17.80±0.04
(15x197) global	-0.86±0.01	0.51±0.04	-0.02±0.01	3.0±0.3	18.40±0.03

Table 4.1: Comparison of the elastic parameters of DNA ($F < 30$ pN) from [32, 37, 38], with those of torsionally unconstrained chromatin fibers (25 repeats), and torsionally constrained chromatin fibers (25 nucleosomes and 15 nucleosomes).

and the data.

4.2.5 Extension-twist curves

Besides pulling the chromatin fiber at constant excess linking numbers, we also twisted the fiber at constant forces similar to experiments by Bancaud et al. [23, 24], but now under conditions that favour higher order folding of chromatin. A comparable response of the fiber to force and twist is evident in the Extension-Twist (E-T) curves, shown in Fig. 4.2A. At high force ($F=3.4$ pN), the fiber's extension hardly changes under negative twist, whereas under positive twist, the extension first increases and reaches a maximum value at $\Delta Lk = 21$, and subsequently decreases symmetrically. At an intermediate force ($F=1.8$ pN), the extension hardly changes under both negative and positive twist in the range of $-20 < \Delta Lk < 40$. At low force ($F=0.4$ pN), fiber shortenes with negative twist, whereas under positive twist, the extension remains constant up to 30 turns. After 30 turns, a decrease in extension occurs with a slope similar to that at negative twist.

When we plot the E-T curves calculated with our model, we obtain excellent agreement at $F > 1.8$ pN. Again, the data can be interpreted as the unfolding of the fiber at sufficient positive twist. Like in the pulling experiment, in the twisting experiment the calculated number of unfolded nucleosomes (Fig. 4.2C) indicates that the nucleosomes

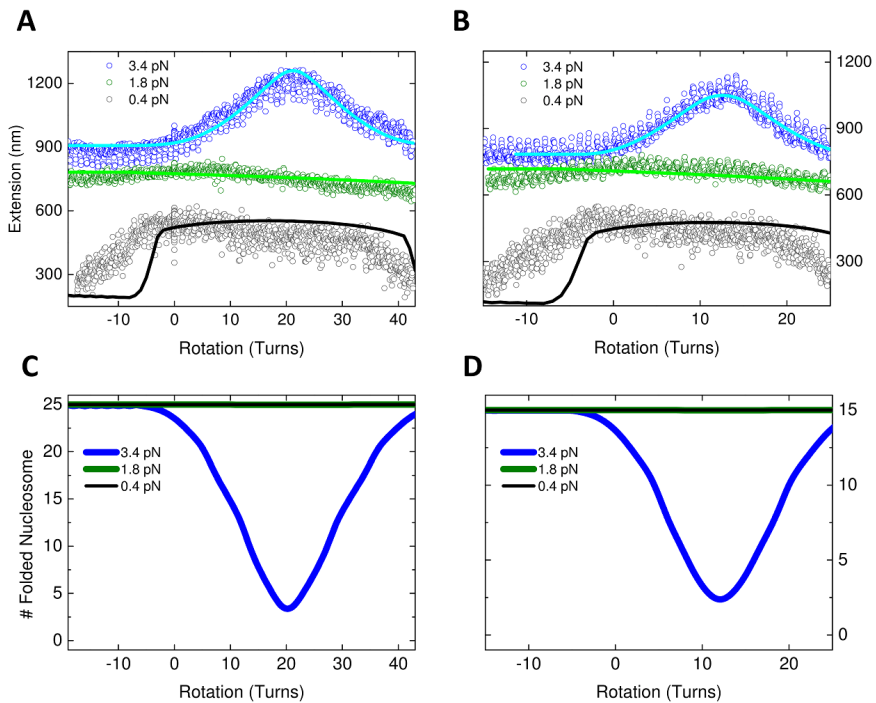


Figure 4.2: Extension versus twist data (dots) at constant force, together with the calculated extension using the parameters from the global fit to the F-E curves shown in Fig. 4.1 and Fig. S3 (solid lines). (A) Fiber reconstituted with 25 nucleosomes. (B) Fiber reconstituted with 15 nucleosomes. (C) and (D) are the calculated number of folded nucleosomes corresponding to (A) and (B).

first unfold from the fiber by increasing positive twist, and subsequently refold when additional positive twist is applied. At 0.4 pN, however, we observe the same discrepancy at negative twist that we found in the F-E data.

Experimental data of the chromatin fiber reconstituted on 15 repeats shows a similar response to force and twist (shown in Fig. 4.2B, Fig. S2,3). The global fit parameters of 15 repeats obtained from the F-E curves are very close to those found for 25 repeats (shown in Table 4.1), which indicates that the model properly takes the number of nucleosome into account. Overall, we get a good agreement between our model and the data, showing that the folded chromatin fiber can be described by a torsional spring with a left-handed chirality. Moreover, the effect of supercoiling on the stability of the fiber is accurately described by taking the mechanical and thermodynamical properties of such a torsional spring and of DNA into account.

4.2.6 Salt effects

In vitro studies have shown that the compaction of chromatin requires divalent ions [3]. We tested the influence of Mg^{2+} on the elasticity of torsionally constrained fibers. All the experiments done in 100 mM K^+ , 2 mM Mg^{2+} , the E-T curves at $F=0.5$ pN show that forward twisting (adding excess linking numbers) and backward twisting (reducing excess linking numbers) curves overlap, indicating that all deformations of the fiber are reversible (Fig. 4.3A). When depleting Mg^{2+} the E-T curves at 0.5 pN hardly change (Fig. 4.3B). This indicates that the structure of the folded fiber is stable, and that Mg^{2+} depletion barely influences the mechanical properties of the folded fiber at low force.

The F-E curves for pulling and releasing at constant linking numbers also overlap in pulling experiments in buffers containing Mg^{2+} , (shown in Fig. 4.3C). This absence of hysteresis indicates that the fiber is in equilibrium during the folding and unfolding events. When the Mg^{2+} is depleted (Fig. 4.3B), F-E curves at $\Delta Lk = 0$ are hardly affected. F-E curves start to differ however, when positive twist is applied. The unfolding transitions above 2.5 pN in Mg^{2+} depleted buffer, show large hysteresis, indicating that an unfolded fiber refolds more slowly than it unfolds without Mg^{2+} . Thus, the effects of torsion are more persistent in the absence of Mg^{2+} .

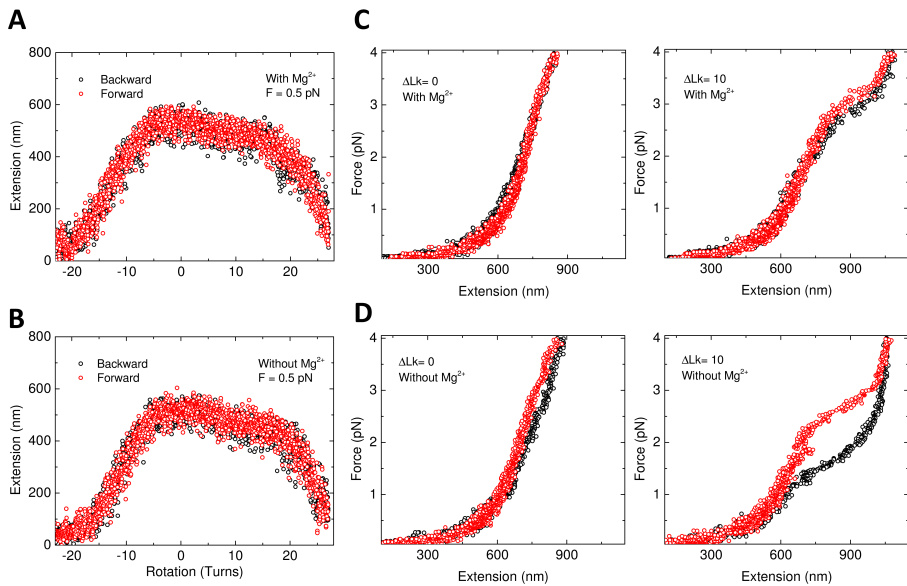


Figure 4.3: Salt dependence of chromatin fiber folding (15 nucleosomes) at different degree of supercoiling. Twist-Extension curves of the fiber at 0.5 pN, with (A) and without Mg^{2+} (B). Both curves show no hysteresis between forward twisting (adding excess linking numbers) and backward twisting (reducing excess linking numbers), indicating that depletion of Mg^{2+} doesn't induce structural changes at this force regime. (C) Pulling and releasing the fiber in 100 mM K^+ and 2 mM Mg^{2+} . The pulling and release traces overlap, indicating the folding and refolding is in equilibrium. (D) Replacing the buffer with 100 mM K^+ without Mg^{2+} . The pulling and release curves show large hysteresis, and irregular refolding and unfolding of the fiber.

4.3 Discussion and conclusions

In this work, we describe the anisotropic elastic response of torsionally constrained chromatin fibers, and quantify this response using a torsional spring model. In combination with the statistical mechanics describing the unfolding of the chromatin fiber, we found that the Hookean torsional spring model accurately describes the fiber's force-dependent extension, regardless of the total number of folded nucleosomes. The obtained fit parameters give a more detailed insight to the structure of chromatin fiber. A linking number per nucleosome $Lk_{fiber}^o \simeq -0.8$ indicates that chromatin fiber has a left-handed chirality.

To evaluate the role of higher order folding of the chromatin fiber, this number can be compared to the amount of supercoiling that is constraint in a single nucleosome. Though one nucleosome contains 1.7 turns of DNA, the linking number of a single nucleosome is only -1 [39, 40]. This difference is known as the linking number paradox [41]. Thus, the contribution of unwrapping the first turn to the change in the linking number is about -0.4. The rest of Lk_{fiber}^o must therefore be attributed to the higher-order structure of fiber that is stabilized by nucleosome-nucleosome and nucleosome-DNA interactions. Our model does not yield a satisfactory global fit to the data if we reduce the excess linking number Lk_{fiber}^o in the free energy term in Equation 4.1 and 4.5 to -0.4. Having two turns per five nucleosomes in the folded chromatin fiber, however, seems excessive. Modeling and EM reconstructions rather suggest about seven nucleosomes per helical twist in a solenoidal fiber, yielding $Lk_{fiber}^o \simeq 0.14$. The remaining part could easily be maintained by undertwisting the linker DNA, which would lead to a twist density of $-0.05 \left(-(0.4 - 0.14) / (50/10.4) \right)$. This is close to the twist densities that are found in vivo. The quantification of the excess linking number that we describe here is therefore fully compatible with a solenoid folding of the chromatin fiber with 50 bp linker DNA.

It is informative to compare our measured elastic parameters of torsionally constrained chromatin fibers with bare DNA and torsionally unconstrained chromatin fibers (Table 4.1). Both the stretch and twist modulus of the folded chromatin fiber are dramatically smaller than those of bare DNA. The small twist modulus, which is about hundred times smaller than that of DNA, implies that a chromatin fiber is very soft and it can absorb large twists without building up much torque. The twist-coupling factor g_f obtained here is a very small number, comparable to the uncertainty in the fit.

This suggests that in this force regime ($F < 4.0$ pN), there is no significant twist-stretch coupling. The low stretch and twist modulus of the fiber that we report here, suggests that large changes in extension and linking number can readily be absorbed by neighboring chromatin within single topological domain. Thus excessive stresses may be effectively prevented by the soft chromatin fiber.

The unfolding energy G_u captures the unfolding transitions of a torsionally constrained fiber in a wide range of twist densities. Moreover, this energy is close to the value that is obtained in independent experiments with torsionally unconstrained chromatin fibers. This indicates that the energy barrier of a nucleosome between the folded and unfolded state of a nucleosome is independent of torsional stress. The change in rupture force that we report here can therefore be fully attributed to the energy associated with twisting the DNA. Recent measurements on the effect of torque on the stability of a mononucleosome [22] qualitatively show that the rupture force for the first turn unwrapping event is increased by positive torque. We tested if our model can quantitatively explain these experimental results. By replacing the fiber with a single nucleosome, leaving out the chirality, the stretch and the twist modulus of the fiber, and simply considering a constant unfolding energy G_u , we are able to reproduce the rupture force-torque relation similar to the experimental results (shown in Fig. S4). This reinforces our model in which we have a strict mechanical coupling between the nucleosomes, and the linker and handle DNA.

In this study we used highly regular, homogeneous chromatin fibers that are known to fold in regular 30-nm structures. In vivo, chromatin is likely to be far less structured, and the existence of such fibers is still heavily debated. We note that all the interactions that we describe here are between neighboring nucleosomes and the unfolding mechanism seems to be conserved over a wide range of linker DNA (20, 55 bp, data not shown). This lack of cooperativity, as demonstrated by the independence of the thermodynamical parameters on the number of nucleosomes in the fiber, indicates that these results can be applied to any pair of nucleosomes. Having a regular chromatin fiber greatly facilitates the interpretation of these nano-mechanical measurements, but we expect that the described mechanical coupling and interaction energies can also be applied to pairs of nucleosomes in irregular chromatin fibers.

Our experiments are conducted under moderate tension and torsion with force smaller than 4 pN, and excess linking number $|\Delta Lk| < 2/\text{nucleosome}$. Under more ex-

Extreme stress conditions, the nucleosome may respond with various chiral transitions [24]. Furthermore, DNA with positive twist and forces larger than 3 pN may transfer into a new conformation, P-DNA [42]. The force and twist regime that we describe here is highly relevant for the situation *in vivo*. The activity of molecular motors, such as RNAP leads to the build up of torsional stress on the DNA. It has been speculated that this stress involves the disassembly and reassembly of chromatin [16, 17], and therefore may be a critical factor to regulate gene transcription. Previous studies reported that RNAP can overcome the obstacle of a nucleosome at $F \sim 4$ pN under torsionally unconstrained conditions [43, 44]. According to the “twin supercoiled domain model” [15], RNAP generates positive twist ahead of transcription direction and negative twist behind. In our experiments, we show that positive supercoiling is readily absorbed by the fiber, which subsequently facilitates fiber unfolding. On the other hand, we show that negative twist can refold and stabilize the fiber. Interestingly, excessive positive twist will drive the nucleosome to refold. This might play a role in the transcription termination in eukaryotes, which is currently poorly understood [45].

In summary, we accurately quantified the elastic properties of a well-defined, folded, torsionally constrained chromatin fiber. The data and modelling suggests that the chromatin fiber folds into a left-handed helix. Both observations support the anticipated role of the “twin supercoiled domain model” in chromatin maintenance. It even suggests that higher-order folding of the fiber may contribute to reinforce this effect. Its anisotropic response to supercoiling may have important implications for all processes involving DNA during the cell cycle.

4.4 Materials and methods

4.4.1 Magnetic tweezers

The home-built magnetic tweezers was described before by Kruithof et al. [46]. During an experiment a DNA or chromatin molecule was constrained between the end of a superparamagnetic bead with diameter of $1 \mu\text{m}$ and the surface of a microscope coverslip. Tension and torsion on the fiber are manipulated by the pair of magnets. Moving the magnets up and down changes the force on the bead. Rotating the magnets changes the degree of supercoiling, i.e., the excess linking number (ΔLk). Each turn changes ΔLk by ± 1 . Supercoiling was induced by rotating the magnets at 1 turn/s. The extension of DNA was measured in real time at a frame rate of 60 Hz with a CCD camera (Pulnix TM-6710CL). No averaging or filtering was used. During experiments, we first twisted

a fiber at low force (0.05 pN) to a desired ΔLk , and then pulled on the fiber. Alternatively, we moved the magnets to a certain position [46] and measured extension versus ΔLk at constant force.

4.4.2 Chromatin constructs

Two DNA constructs with 25 or 15 tandem repeats of the 601 sequence were used based on Puc18 (A gift from D. Rhodes, Singapore). Both plasmids were digested with BsaI and BseYI yielding linear fragments of 2410 and 6960 bp with corresponding sticky ends. Digoxigenin and biotin-labeled handles were produced with PCR using 10% biotin-dUTP and digoxigenin-dUTP on the pGem-3Z template using the following primers: 5' GAT AAA TCT GGA GCC GGT GA 3' and 5' CTC CAA GCT GGG CTG TGT 3'. After PCR amplification, the fragments were digested with BsaI and BseYI and ligated to the previously digested DNA 601 array. The ligation product was mixed with competitor DNA (-147 bp) and histone octamers purified from chicken erythrocytes, and reconstituted into chromatin fibers using salt dialysis [47].

4.4.3 Sample preparation

A clean cover slip was coated with 1% polystyrene-toluene solution. The cover slip was then mounted on a poly-di-methylsiloxane (PDMS, Dow Corning) flow cell containing a $10 \times 40 \times 0.4$ mm flow channel. The flow cell was incubated with 1 $\mu\text{g/ml}$ anti-digoxigenin for 2 hours and 2% BSA (w/v) solution over night. 20 ng/ml DNA folded into chromatin in 10 mM HEPES, pH 7.6, 100 mM KAc and 10 mM NaN_3 was flushed into the flow cell and incubated for 10 minutes, followed by flushing in 1 μm streptavidin-coated superparamagnetic microspheres (MyOne, Invitrogen) diluted one thousand times in the same buffer. After 10 minutes excess beads were flushed away using the same buffer.

4.5 Supplemental Information

4.5.1 Variables and derived expressions

Below, we use the following parameters to describe the mechanical properties of DNA:

F = Force;

A_t = Bending persistence length (50 nm for twisted DNA);

$k_B T$ = Thermal energy;

$C_t = C \left(1 - \frac{C}{4A_t} \sqrt{\frac{k_B T}{A_t F}} \right)$ = Twist persistent length as a function of force (twisted DNA)

, with constant $C = 100$ nm;

C_p = Twist persistent length of plectonemic DNA (24 nm for plectonemic DNA);

L_o = Contour length;

$g = \left(F - \sqrt{\frac{F k_B T}{A_t}} \right)$ = Free energy per nm of torsionally unconstrained DNA.

4.5.2 Elasticity of supercoiled DNA

A supercoiled DNA molecule can be described by 3 different conformations, i.e, twisted, plectonemic, and melted states. The free energy of twisted DNA is given by a parabola function ($G'_{DNA} = G_{DNA} - Fz_{DNA}$) [35, 48] :

$$G'_{DNA} = L_o \left(-g + \frac{k_B T C_t}{2} \left(\frac{2\pi \Delta L k_{DNA}}{L_o} \right)^2 \right). \quad (4.7)$$

The extension of twisted DNA is calculated by taking the derivative of free energy to force:

$$z_{DNA} = -\frac{dG'_{DNA}}{dF} = L_o \left(1 - \frac{1}{2} \sqrt{\frac{k_B T}{A_t F}} - \frac{C^2}{16} \left(\frac{2\pi \Delta L k_{DNA}}{L_o} \right)^2 \left(\frac{k_B T}{A_t F} \right)^{\frac{3}{2}} \right). \quad (4.8)$$

As twist is applied to the DNA, the restoring torque will increase linearly with the excess linking number it absorbed, before any conformational changes:

$$\Gamma_{DNA} = C_t \frac{2\pi \Delta L k_{DNA}}{L_o} k_B T. \quad (4.9)$$

4.5.3 Positive supercoiling: plectonemic and twisted DNA

DNA under positive twist can be overwound, staying in a twisted conformation or transform into plectonemic conformation. An analytical solution yielded a constant torque when the DNA buckles into plectonemic states [35]:

$$\Gamma_c^+ = \sqrt{\frac{2k_B T C_p g}{1 - C_p/C_t}}. \quad (4.10)$$

The maximum linking number that can be absorbed by DNA before conformation change is then:

$$\Delta L k_{\max}^+ = \Gamma_c^+ L_o / (2\pi k_B T C_t) \quad (4.11)$$

The total extension of DNA after buckling decreases linearly by increasing linking numbers, the slope in nm/turn is given by [35, 37]:

$$\Delta z_{DNA} = \frac{2\pi \left[1 - \frac{1}{2} \sqrt{\frac{k_B T}{A_t F}} - \frac{C^2}{16 C_t^2} \left(\frac{k_B T}{A_t F} \right)^{3/2} \left(\frac{\Gamma_c^+}{k_B T} \right)^2 \right]}{\frac{\Gamma_c^+}{k_B T} \left(\frac{1}{C_p} - \frac{1}{C_t} \right)} \quad (4.12)$$

The free energy of DNA will increase linearly; the gain in free energy per turn is:

$$\Delta G_{DNA}^+ = 2\pi \Gamma_c^+ \quad (4.13)$$

4.5.4 Negative supercoiling: plectonemic, melted and twisted DNA

DNA under negative twist can stay in the twisted state, or can have conformational change to become melted or plectonemic DNA. Without the existence of melted DNA, the mechanical properties of negative supercoiled DNA are identical to those for positive supercoiling. When we consider the coexistence of twisted and melted states, the constant torque is limited due to melting [36]:

$$\Gamma_c^- = -11 pN nm \quad (4.14)$$

To solve the problem of the different possible conformations of the DNA, we consider two scenarios. If the calculated buckling torque in Equation 4.10 is smaller than the constant torque in Equation 4.14, then the DNA coexists in twisted and plectonemic states; if the calculated buckling torque in Equation 4.10 exceeds -11 pN nm, DNA

exists in twisted and melted states. The maximum linking number DNA can absorb before conformation change is then:

$$\Delta Lk_{\max}^- = \Gamma_c^- L_o / (2\pi k_B T C_t) \quad (4.15)$$

The extension of DNA in the melted state is considered as the same as that of twisted DNA under small degrees of supercoiling, due to the small fraction of melted DNA. The free energy of DNA increases per turn:

$$\Delta G_{DNA}^- = 2\pi \Gamma_c^- \quad (4.16)$$

4.5.5 The analytical solution of a DNA-fiber tether

Having discussed the mechanical properties of the torsional spring in the main text, the extension and torque of the fiber are expressed as:

$$\begin{aligned} \Delta z_{fiber} &= \frac{F - g'_f 2\pi Lk_{fiber}}{s'_f} \\ \Gamma_{fiber} &= c'_f 2\pi Lk_{fiber} + g'_f \Delta z_{fiber} \end{aligned} \quad (4.17)$$

Here, $s'_f = s_f / Nz_f^o$, $g'_f = g_f / Nz_f^o$ and $c'_f = c_f / Nz_f^o$. Equating the torque in the fiber and in the DNA, and considering the total excess linking number is distributed between the DNA and the fiber, we find:

$$\begin{aligned} \Delta Lk &= \Delta Lk_{DNA} + \Delta Lk_{fiber} \\ Lk_{fiber} &= N \times Lk_{fiber}^o + \Delta Lk_{fiber} \\ c'_f 2\pi Lk_{fiber} + g'_f \times \frac{F - g'_f 2\pi Lk_{fiber}}{s'_f} &= C_t \frac{2\pi \Delta Lk_{DNA}}{L_o} k_B T \end{aligned} \quad (4.18)$$

Solving Equation 4.18 yields

$$\begin{aligned} \Delta Lk_{DNA} &= - \frac{2\pi N s'_f c'_f Lk_{fiber}^o + g'_f (F - 2\pi N g'_f Lk_{fiber}^o) - 2\pi ((g'_f)^2 - s'_f c'_f) \Delta Lk}{2\pi \left((g'_f)^2 - s'_f c'_f - \frac{s'_f k_B T}{L_o} C_t \right)} \\ \Delta Lk_{fiber} &= \Delta Lk - \Delta Lk_{DNA} \end{aligned} \quad (4.19)$$

After plectonemic or melted states form in the DNA, we compare Equation 4.19 with Equation 4.11 and 4.15. For large excess linking numbers the torque will stay constant at Γ_c^\pm and the linking number distribution is then given by:

$$\Delta Lk_{fiber} = \frac{Fg'_f - s'_f \Gamma_c^\pm}{2\pi((g'_f)^2 - s'_f c'_f)} - N \times Lk_{fiber}^o \quad (4.20)$$

$$\Delta Lk_{DNA} = \Delta Lk - \Delta Lk_{fiber}$$

The extension of the tether at a certain force and excess linking number can now be calculated as:

$$z(F, \Delta Lk, N) = z_{DNA}(F, \Delta Lk_{DNA}) + z_{fiber}(F, \Delta Lk_{fiber}, N) \quad (4.21)$$

The extension of DNA is considered for all the three states, twisted, plectonemic and melted states by using Equation 4.8 and 4.12. When the unfolding of the chromatin fiber is considered, as discussed in the main text, the partition function is written in the terms of free energy:

$$Z = \sum_{i=0}^N \binom{N}{i} \exp\left(-\frac{G_{DNA} + G_{fiber} + iG_u - Fz(F, \Delta Lk + iLk_{fiber}^o, i)}{k_B T}\right) \quad (4.22)$$

One should notice the free energy of the DNA is $G_{DNA} = G'_{DNA} + Fz_{DNA}$ as shown in Equation 4.7. Using the partition function, we calculate the expected values of the parameters that we are interested in.

4.5.6 Supporting figures

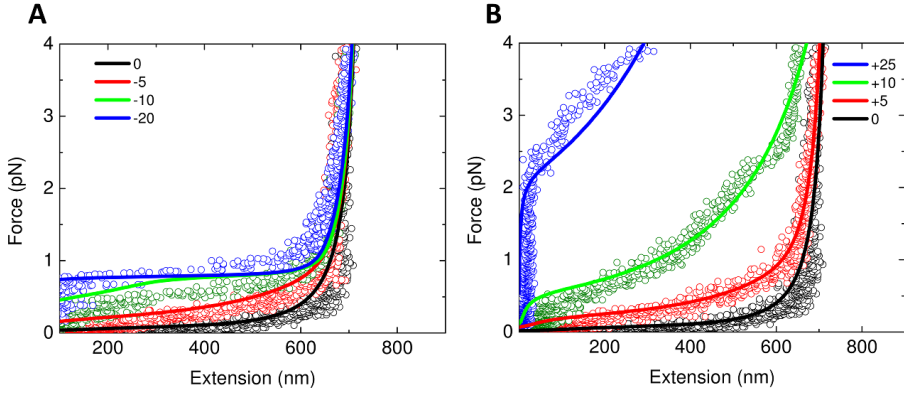
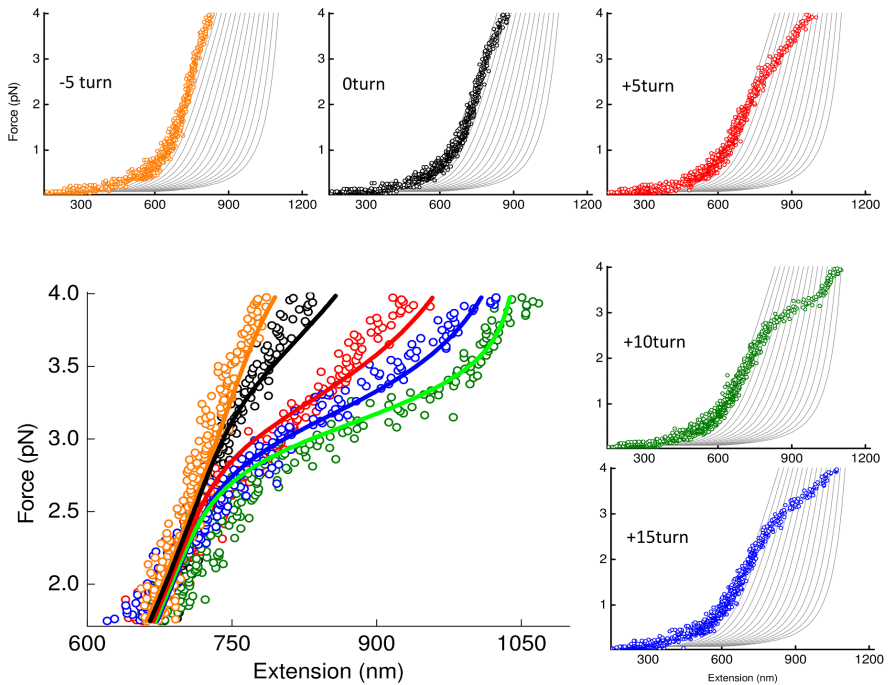


Figure S1

Force-Extension curves of torsionally constrained 2.4 kb DNA under negative supercoiling (A) and positive supercoiling (B). The solid lines are the calculation results by using Equations 4.8-4.15, which is similar to the numerical solution presented in [36]. Under negative twist, the extension of the molecule decreased when increasing the degree of supercoiling at forces below 1.0 pN. Above 1.0 pN, the extension of supercoiled DNA converged to the extension of DNA without twist. Under positive twist, the extension of the molecule decreased when increasing the degree of supercoiling up to $F=4.0$ pN.

**Figure S2**

The force-extension curves of 197x15 repeats torsional constrained chromatin fiber. The global fit results for the five curves from 1.0 pN to 4.0 pN are shown as solid lines. The gray lines as background in each curve are the calculation results of torsionally unconstrained model by varying the number of folded nucleosome as references to the experimental data.

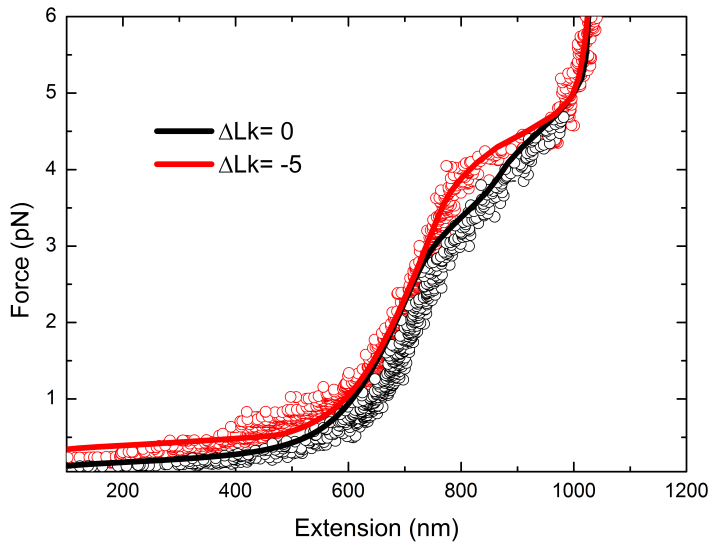
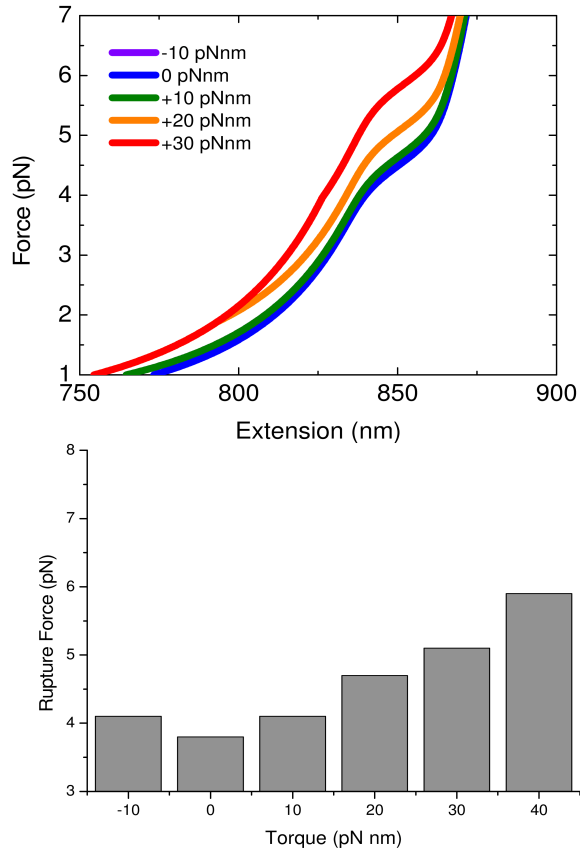


Figure S3

Force-extension curves of 197x15 repeats torsional constrained chromatin fiber with force up to 6 pN by using the magnetic bead with diameter $2.8 \mu m$ instead of $1.0 \mu m$. It shows that under negative twist, around 4 pN the force-extension curve has a force plateau similar to the torsional unconstrained fiber at lower force. Solid lines are the calculations by using the parameters from global fit in main text Table 4.1. It shows a good agreement to the experimental data.

**Figure S4**

Simulated Force-extension curves for a mononucleosome under constant torque. By using our statistical mechanics model discussed in the main text, we decrease the number of nucleosomes to one, and we only use one parameter, the unfolding energy $G_u = 10 k_B T$ to describe the mononucleosome. We converted the excess linking number to torque using Equation 4.9. The calculated curves and rupture forces give the same trend as reported in [22].

References IV

- [1] Watson, J., and F. Crick. 1953. Molecular Structure of Nucleic Acids. *Nature*. 171:737–738.
- [2] Luger, K., A. W. Ma, R. K. Richmond, D. F. Sargent, and T. J. Richmond. 1997. Crystal structure of the nucleosome core particle at 2.8 Å resolution. *Nature*. 389:251–260.
- [3] Li, G., and D. Reinberg. 2011. Chromatin higher-order structures and gene regulation. *Current opinion in genetics & development*. 21:175–86.
- [4] Luger, K., M. L. Dechassa, and D. J. Tremethick. 2012. New insights into nucleosome and chromatin structure: an ordered state or a disordered affair? *Nature reviews. Molecular cell biology*. 13:436–47.
- [5] Bassett, A., S. Cooper, C. Wu, and A. Travers. 2009. The folding and unfolding of eukaryotic chromatin. *Current opinion in genetics & development*. 19:159–65.
- [6] Grigoryev, S. a., and C. L. Woodcock. 2012. Chromatin organization - the 30 nm fiber. *Experimental cell research*. 318:1448–55.
- [7] Eltsov, M., K. M. Maclellan, K. Maeshima, A. S. Frangakis, and J. Dubochet. 2008. Analysis of cryo-electron microscopy images does not support the existence of 30-nm chromatin fibers in mitotic chromosomes in situ. *Proceedings of the National Academy of Sciences of the United States of America*. 105:19732–7.
- [8] Maeshima, K., S. Hihara, and M. Eltsov. 2010. Chromatin structure: does the 30-nm fibre exist in vivo? *Current opinion in cell biology*. 22:291–7.
- [9] Nishino, Y., M. Eltsov, Y. Joti, K. Ito, H. Takata, Y. Takahashi, S. Hihara, A. S. Frangakis, N. Imamoto, T. Ishikawa, and K. Maeshima. 2012. Human mitotic chromosomes consist predominantly of irregularly folded nucleosome fibres without a 30-nm chromatin structure. *The EMBO journal*. 31:1644–53.
- [10] Fudenberg, G., and L. a. Mirny. 2012. Higher-order chromatin structure: bridging physics and biology. *Current opinion in genetics & development*. 22:115–24.
- [11] Naumova, N., M. Imakaev, G. Fudenberg, Y. Zhan, B. R. Lajoie, L. a. Mirny, and J. Dekker. 2013. Organization of the mitotic chromosome. *Science*. 342:948–53.

-
- [12] Li, B., M. Carey, and J. L. Workman. 2007. The role of chromatin during transcription. *Cell*. 128:707–19.
- [13] Brooks, T. a., and L. H. Hurley. 2009. The role of supercoiling in transcriptional control of MYC and its importance in molecular therapeutics. *Nature reviews. Cancer*. 9:849–61.
- [14] Darzacq, X., Y. Shav-Tal, V. de Turris, Y. Brody, S. M. Shenoy, R. D. Phair, and R. H. Singer. 2007. In vivo dynamics of RNA polymerase II transcription. *Nature structural & molecular biology*. 14:796–806.
- [15] Wang, J. C., and A. S. Lynch. 1993. Transcription and DNA supercoiling. *Current opinion in genetics & development*. 3:764–8.
- [16] Clark, D. J., and G. Felsenfeld. 1992. A nucleosome Core Is Transferred out of the Path of a Transcribing polymerase. *Cell*. 71:11–22.
- [17] Teves, S. S., and S. Henikoff. 2014. Transcription-generated torsional stress destabilizes nucleosomes. *Nature structural & molecular biology*. 21:88–94.
- [18] Naughton, C., N. Avlonitis, S. Corless, J. G. Prendergast, I. K. Mati, P. P. Eijk, S. L. Cockroft, M. Bradley, B. Ylstra, and N. Gilbert. 2013. Transcription forms and remodels supercoiling domains unfolding large-scale chromatin structures. *Nature structural & molecular biology*. 20:387–95.
- [19] Kouzine, F., A. Gupta, L. Baranello, D. Wojtowicz, K. Ben-Aissa, J. Liu, T. M. Przytycka, and D. Levens. 2013. Transcription-dependent dynamic supercoiling is a short-range genomic force. *Nature structural & molecular biology*. 20:396–403.
- [20] Ma, J., L. Bai, and M. D. Wang. 2013. Transcription under torsion. *Science*. 340:1580–3.
- [21] Gilbert, N., and J. Allan. 2014. Supercoiling in DNA and chromatin. *Current Opinion in Genetics & Development*. 25:15–21.
- [22] Sheinin, M. Y., M. Li, M. Soltani, K. Luger, and M. D. Wang. 2013. Torque modulates nucleosome stability and facilitates H2A/H2B dimer loss. *Nature communications*. 4:2579.

- [23] Bancaud, A., N. Conde e Silva, M. Barbi, G. Wagner, J.-F. Allemand, J. Mozziconacci, C. Lavelle, V. Croquette, J.-M. Victor, A. Prunell, and J.-L. Viovy. 2006. Structural plasticity of single chromatin fibers revealed by torsional manipulation. *Nature structural & molecular biology*. 13:444–50.
- [24] Bancaud, A., G. Wagner, N. Conde E Silva, C. Lavelle, H. Wong, J. Mozziconacci, M. Barbi, A. Sivolob, E. Le Cam, L. Mouawad, J.-L. Viovy, J.-M. Victor, and A. Prunell. 2007. Nucleosome chiral transition under positive torsional stress in single chromatin fibers. *Molecular cell*. 27:135–47.
- [25] Kruithof, M., F.-T. Chien, A. Routh, C. Logie, D. Rhodes, and J. van Noort. 2009. Single-molecule force spectroscopy reveals a highly compliant helical folding for the 30-nm chromatin fiber. *Nature structural & molecular biology*. 16:534–40.
- [26] Victor, J. M., J. Zlatanova, M. Barbi, and J. Mozziconacci. 2012. Pulling chromatin apart: Unstacking or Unwrapping? *BMC biophysics*. 5:21.
- [27] Williams, S. P., B. D. Athey, L. J. Muglia, R. S. Schappe, H. Albert, and J. P. Langmore. 1986. Chromatin fibers are left-handed double helices with diameter and mass per unit length that depend on linker length. *Biophysical journal*. 49:233–245.
- [28] Marko, J. 1997. Stretching must twist DNA. *Europhysics Letters*. 38:183–188.
- [29] Bustamante, C., S. B. Smith, J. Liphardt, and D. Smith. 2000. Single-molecule studies of DNA mechanics. *Current opinion in structural biology*. 10:279–85.
- [30] Strick, T. R., J. F. Allemand, D. Bensimon, A. Bensimon, and V. Croquette. 1996. The elasticity of a single supercoiled DNA molecule. *Science*. 271:1835–7.
- [31] Strick, T. R., J. F. Allemand, D. Bensimon, and V. Croquette. 1998. Behavior of supercoiled DNA. *Biophysical journal*. 74:2016–28.
- [32] Gore, J., Z. Bryant, M. Nöllmann, M. U. Le, N. R. Cozzarelli, and C. Bustamante. 2006. DNA overwinds when stretched. *Nature*. 442:836–9.
- [33] Durickovic, B., A. Goriely, and J. H. Maddocks. 2013. Twist and Stretch of Helices Explained via the Kirchhoff-Love Rod Model of Elastic Filaments. *Physical Review Letters*. 111:108103.

-
- [34] Robinson, P. J. J., W. An, A. Routh, F. Martino, L. Chapman, R. G. Roeder, and D. Rhodes. 2008. 30 nm chromatin fibre decompaction requires both H4-K16 acetylation and linker histone eviction. *Journal of molecular biology*. 381:816–25.
- [35] Marko, J. 2007. Torque and dynamics of linking number relaxation in stretched supercoiled DNA. *Physical Review E*. 76:021926.
- [36] Meng, H., J. Bosman, T. van der Heijden, and J. van Noort. 2014. Coexistence of Twisted, Plectonemic, and Melted DNA in Small Topological Domains. *Biophysical Journal*. 106:1174–1181.
- [37] Forth, S., C. Deufel, M. Sheinin, B. Daniels, J. Sethna, and M. Wang. 2008. Abrupt Buckling Transition Observed during the Plectoneme Formation of Individual DNA Molecules. *Physical Review Letters*. 100:148301.
- [38] Gross, P., N. Laurens, L. B. Oddershede, U. Bockelmann, E. J. G. Peterman, and G. J. L. Wuite. 2011. Quantifying how DNA stretches, melts and changes twist under tension. *Nature Physics*. 7:731–736.
- [39] Simpson, R. T., F. Thoma, and J. M. Brubaker. 1985. Chromatin reconstituted from tandemly repeated cloned DNA fragments and core histones: a model system for study of higher order structure. *Cell*. 42:799–808.
- [40] Hayes, J. J., T. D. Tullius, and a. P. Wolffe. 1990. The structure of DNA in a nucleosome. *Proceedings of the National Academy of Sciences of the United States of America*. 87:7405–9.
- [41] Prunell, A. 1998. A topological approach to nucleosome structure and dynamics: the linking number paradox and other issues. *Biophysical journal*. 74:2531–44.
- [42] Allemand, J. F., D. Bensimon, R. Lavery, and V. Croquette. 1998. Stretched and overwound DNA forms a Pauling-like structure with exposed bases. *Proceedings of the National Academy of Sciences of the United States of America*. 95:14152–7.
- [43] Hodges, C., L. Bintu, L. Lubkowska, M. Kashlev, and C. Bustamante. 2009. Nucleosomal fluctuations govern the transcription dynamics of RNA polymerase II. *Science*. 325:626–8.
- [44] Bintu, L., T. Ishibashi, M. Dangkulwanich, Y.-Y. Wu, L. Lubkowska, M. Kashlev, and C. Bustamante. 2012. Nucleosomal elements that control the topography of the barrier to transcription. *Cell*. 151:738–49.

- [45] Kuehner, J. N., E. L. Pearson, and C. Moore. 2011. Unravelling the means to an end: RNA polymerase II transcription termination. *Nature reviews. Molecular cell biology*. 12:283–94.
- [46] Kruithof, M., F. Chien, M. de Jager, and J. van Noort. 2008. Subpiconewton dynamic force spectroscopy using magnetic tweezers. *Biophysical journal*. 94:2343–8.
- [47] Routh, A., S. Sandin, and D. Rhodes. 2008. Nucleosome repeat length and linker histone stoichiometry determine chromatin fiber structure. *Proceedings of the National Academy of Sciences of the United States of America*. 105:8872–7.
- [48] Tinoco, I., and C. Bustamante. 2002. The effect of force on thermodynamics and kinetics of single molecule reactions. *Biophysical chemistry*. 101-102:513–33.